Annals of R.S.C.B., ISSN:1583-6258, Vol. 25, Issue 4, 2021, Pages. 12822 - 12833
Received 05 March 2021; Accepted 01 April 2021.

Preparation and Characterization of Hyaluronic Acid/ Hydroxyapatite Composite (HA/HAp) Scaffolds for Bone Tissue Engineering

FathimaShahithaJahirHussain[1], Mohammed Al-Sibani[2], AsiyaObaidAbdallah Al Saadi[3]
[1,2,3]The College of Arts and Sciences, University of Nizwa Initial Campus, Birkat Al Mouz, P.O. Box 33, PC 616, Nizwa, Sultanate of Oman

ABSTRACT

Three dimensional biodegradable porous polymer/ hydroxyapatite scaffolds play vital role in tissue engineering. This study is focused to develop a highly porous biocompatible composite scaffold using hyaluronic acid (HA) and Hydroxyapatite (HAp). The hyaluronic acid (HA) sponges cross-linked with 1, 4-butanediol diglycidyl ether (BDDE) were synthesized using freeze-drying technique and the mineralization of hydroxyapatite on the HA sponges were carried out by immersing the HA sponges in the simulated body fluid (SBF) solution for various period of time. The morphology of HA/HAp composites were studied using scanning electron microscopy (SEM) and the presence of hydroxyapatite was confirmed by energy dispersive X-ray (EDX) studies. The chemical and thermal properties were studied using ATR-FTIR and TGA studies respectively. The results showed that the HA/HAp composites had an open porous structure with pore size in the range of 30–300 μm. Most of the composites showed excellent porosity above 90%, which is an important requirement for tissue engineering applications. The hydroxyapatite crystals were polygonal shaped with sizes in the range of 0.5-5.0 μm. The possible chemical interaction between HA andHAp was confirmed by FTIR. The mass loss of HA/HAp composites were shown by TGA curves. These results suggest that the HA/HAp composite scaffolds fabricated by freeze-drying method might be a suitable biomaterial for bone tissue engineering applications.

Introduction

Tissue engineering involving glycosaminoglycans (GAGs) are extremely promising due to their excellent bioactivity including cell adhesion, proliferation and non-toxicity, leading to scaffolds which mimic the extra cellular matrix.[1] Numerous biomaterials have been developed using (GAGs) to improve the human life that are used as implants in different dysfunctions like, atherosclerotic arteries, decaying teeth and arthritic hips.[2] Several types of (GAGs) are widely studied including, hydroxyethyl cellulose, heparin, keratin sulphate, hyaluronic acid and so on.[1, 3,4]

Hyaluronic acid (HA) is a high molecular weight poly-anionic glycosaminoglycan with excellent water retention property, found in various body tissues supporting their structural and physiological characteristics. HA is also the primary extra cellular matrix (ECM) component of brain tissue. HA has repeating disaccharide units of glucuronic acid and N-acetyl-D-glycosamine linked by alternating glycosidic bonds β-(1,4) and β-(1,3) and can interact with various specific binding proteins.[5] HA has showed special role in the formation of ossification centres, skeletal growth in the developing limb and tibial growth plate.[6] Hyaluronic acid alone is used as a scaffold[7] or mixed with various polymers and inorganic materials to form composites like HA, chitosan/collagen sponges with calcium phosphate,[8] HA/aragonite[1], HA/silk fibroin[9], HA/ collagen and EDAC/NHS,[10] HA/ silk fibroin and chondroitin,[11] HA/ chitosan.[12] A perfect inorganic material in composite scaffolds for bone substitute is hydroxyapatite which has excellent osteo conductivity, bioactivity and biocompatibility.[13] Calcium hydroxyapatite initiates the mineralization process and also reported to improve the cell response to the implanted material.

Scaffolds in tissue engineering are fabricated by various techniques including self-assembly electro-spinning, freeze-drying, phase separation, solvent casting and particulate leaching (SCPL).[14-17] Freeze-drying technique is widely used to produce scaffolds with various sizes of

Annals of R.S.C.B., ISSN:1583-6258, Vol. 25, Issue 4, 2021, Pages. 12822 - 12833
Received 05 March 2021; Accepted 01 April 2021.

interconnected pores. Highly porous structure is obtained by this low temperature dehydration process which removes most of the water from the sample under vacuum.

Porous HA exhibits strong bonding to the bone, the pores provide a mechanical interlock leading to a firm fixation of the material. Bone tissue grows well into the pores, thus increasing strength of the HA implant. A porous hydroxyapatite coating facilitates bone growth through a highly convoluted interface. When pore sizes exceed 100 μm, bone grows through the channels of interconnected surface pores, thus maintaining the bone's vascularity and viability.[18]Various polymer/ hydroxyapatite composites have been studies including collagen/Hap, chitosan, collagen, and hyaluronic acid with hydroxyapatite[19] but so far there is no report on hyaluronic acid mineralized with hydroxyapatite. Usually hyaluronic acid is cross linked with 1,4-butanedioldiglycidyl ether (BDDE) in order to make it water insoluble and improve their stability in aqueous environment as well as to improve their mechanical stability. These polymers with soft character can be used in non-load bearing bone regeneration strategies. Therefore, this study aims to develop composite scaffolds from HA and HAp using freeze-drying technique. This study contributes to the understanding of the effect of in-situ mineralization time in SBF solution on the porosity, thermal and chemical properties of HA cross linked by BDDE.

2. Experimental section

2.1. Materials

All materials used in this work are commercially available. The sodium salt of hyaluronic acid was obtained from VivatisPharma (SWY Biotech Co., Ltd , China), with an average molecular weight 500,000 Da. For synthesis and de-polymerization: 1, 4-butanediol diglycidyl ether (BDDE) and hyaluronidase powder (3000 U/ mg) were purchased from SWY Biotech Co., Ltd , China). NaOH and NaCl were purchased from (SDF CL, sd fine- Chem Limited, India). KCl, $CaCl_2.2H_2O$, HCl and $MgCl_2.6H_2O$ were purchased (Research –lab fine Chem Industries , India) $NaH_2PO_4.2H_2O$ and $NaHCO_3$ were purchased from Scharlau (ScharlauChemieS.A.,European). All the chemicals were of highest purity and used without further purification. All the solutions were prepared using Millipore water.

2.2. Preparation of cross-linked hydrogels

Cross linked hydrogels were prepared by adding 200 μl of 1,4-butanediol diglycidyl ether (BDDE) into 9.8 ml of 0.25 M NaOH, (pH 13). 1.0 g of HA powder was added to the above solution and mixed thoroughly at 40 °C for 2 h and then neutralized with 0.1 M HCl to a pH of approximately 7.0.

The hydrogels were then dialyzed for two days against distilled water to remove BDDE residue and non-reacted HA fragments. The cross-linked hydrogels were then lyophilized using ((MDF-DU900V-PE, Panasonic Healthcare Co., Ltd , Japan.); the samples were first frozen at −80 °C in an ultra-low temperature freezer (MDF-U3386S, SANYO Electric Co., Japan) for 4 h to ensure complete freezing and then sublimed at −50 °C for 24 h under a vacuum of 5 mTorr. When all free ice was removed, the temperature was increased to 25 °C and the samples were left for 2 h to remove trace water molecules bound to them. The schematic is shown in figure 1.

Annals of R.S.C.B., ISSN:1583-6258, Vol. 25, Issue 4, 2021, Pages. 12822 - 12833
Received 05 March 2021; Accepted 01 April 2021.

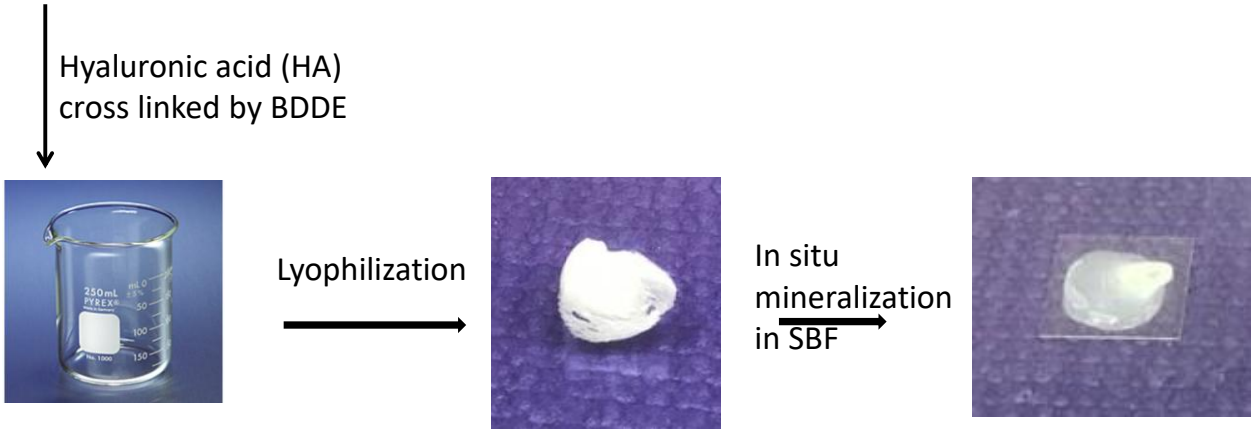

Figure 1. Scheme of HA/HAp composite preparation

2.3. Preparation of simulated body fluids (SBF) and mineralization of HA sponges

The 10x simulated body fluid solutions were prepared according to Tas and Bhaduri[20] and Mavis et al.[21] The chemical composition of 10x SBF solutions is listed in Table 1. All the chemicals are reagent grade. The stock solution was prepared by adding the first five chemicals (Table 1) until complete dissolution of each reagent in 900mL de-ionized water by continuous stirring at room temperature. After the dissolution of the five chemicals, the volume of stock solution was made up to1000mL and stored at room temperature in capped glass bottle for several months without any precipitation. Before the scaffold mineralization, 200 mL of the stock solution was transferred into a beaker and 0.168 g of $NaHCO_3$ was added to the above solution. The pH of the SBF solution was maintained at 7.0. 50 mL of this solution was transferred to a 100 mL glass bottle and 1cm HA sponges was immersed in the solution for 3h, 6h, 12h and 18h at room temperature, after which they were rinsed with de-ionized water to remove the salt residues.[22]

Table 1
Reagents for preparing 1 L of 10x SBF solution.[22]

S.N0	Reagent	Amount (g)	Molarity (mM)
1	NaCl	58.443	1000
2	KCl	0.373	5
3	$CaCl_2 2H_2O$	3.675	25
4	$MgCl_2 6H_2O$	1.016	5
5	$NaH_2PO_4 2H_2O$	0.250	3.62
6	$NaHCO_3$	0.840	10

The comparison of the ionic concentration of the elements between the blood plasma and SBF solution is shown in Table 2.

Table 2

Ionic concentration (mM)	Na^+	K^+	Ca^{2+}	Mg^{2+}	$HCO3^-$	Cl^-	$HPO4^-$	$SO4^{2-}$
Blood plasma	142	5	2.5	1.5	27	103	1	0.5
SBF	142	5	2.5	1.5	4.2	148	1	0.5

Annals of R.S.C.B., ISSN:1583-6258, Vol. 25, Issue 4, 2021, Pages. 12822 - 12833
Received 05 March 2021; Accepted 01 April 2021.

2.4. Porosity study

The porosity of the HA/HAp scaffolds was measured using water displacement method. The scaffolds were cut in 1 cm × 1 cm × 1 cm sizes and immersed in a known volume (V1) of water in a Falcon tube for 30 min. The total volume of water and the water impregnated scaffold was recorded as V2. The water-impregnated scaffolds were then removed from the Falcon tube and the residual water volume was recorded as V3. Experiments were carried out in six replicates for all types of scaffolds. The porosity of the scaffolds was obtained in Eq. (1):[3]

$$\text{Porosity } \% = \frac{V1-V3}{V2-V3} \times 100\%$$

2.5. Characterization

2.5.1. Scanning electron microscope (SEM) study

The microstructures of porous scaffolds were characterized by Scanning Electron Microscopy (SEM) (JEOL JSM 6510LA, Japan) at an accelerating voltage of 15 kV. The dried scaffolds were sputter coated with a thin layer of platinum in double 30 s consecutive cycles at 45 mA to reduce charging and produce conductive surfaces (JEOL, JFC-1600, Japan). The pore sizes were measured manually.

2.5.2 Porosity of scaffolds

Porosity measurements of the HA/HAp sponges were completed by using liquid displacement method with millipore water as a displacement liquid.

2.5.3. ATR-FTIR analysis

ATR-FTIR spectroscopic analysisof HA/HAp sponges was performed on Spectrum One (Bruker, USA) spectrophotometer over a range of 400 to 4000 cm−1 at a resolution of 2 cm−1 with 100 scans per sample.

2.5.4. TGA study

TGA was performed using (SDT Q600 V20.9) where about 5 mg of sample was heat treated from 30 to 750 °C at a heating rate of 10 °C/min with nitrogen as purge gas.

2.5.5. X-ray diffraction study

XRD is a useful method toinvestigate the crystallinity and to determine the obtained phases for the prepared scaffolds. The XRD measurements were carried out using powder X-ray diffraction, model D8Discover. The selected samples were milled in an agate mortar before measuring. XRD patterns of the specimens were examined by utilizing Cukα = 1.54056 A° radiation. The applied current and voltage were 40 mA and 40 kV. XRD was taken at 2Ɵ angle range of 10–80 and the operation condition was scan move size 0.02 (2Ɵ) and scan move time 1 s.

3. Results and discussions

3.1. Scanning electron microscopy (SEM) with energy dispersive X-ray spectroscopy (EDX)

The microstructures of pure HA and the mineralized HA that was immersed in SBF solution at different periods of time are illustrated as in Figure 2. The size and shape of the pores on the scaffold together with the porosity play a very important role in tissue engineering.[23] All the sponges showed porous structure with interconnected pores. These type of materials are very important in tissue engineering since the nutrients flow easily inside the pores and help in the cell proliferation homogeneously on the surface and the inside region of the scaffolds.[24] The HAp crystals were observed on the surface of the HA sponges as well as the inner surface of the pores. This shows that the crystallization has been carried out homogeneously for the entire volume of the HA sponges by this in-situ method. The SEM images of the HA/HAp sponges showed that the pore size were in the range of 100-300 μm and the size of the crystals were in the range of 0.5-5.0 μm. The crystals were polygonal in shape, with rectangle and square shape being

Annals of R.S.C.B., ISSN:1583-6258, Vol. 25, Issue 4, 2021, Pages. 12822 - 12833
Received 05 March 2021; Accepted 01 April 2021.

dominant. Increase in the immersion time in SBF solution did not result in the increase in size of the hydroxyapatite crystals but the amounts of the crystals were increased. The results show that even with 3 h of immersion it is possible to get hydroxyapatite crystals in the range of 0.5-5.0 µm. Overall, these results suggests that the HA/HAp sponges with this pore size can serve as an excellent scaffolds for tissue engineering.[25]

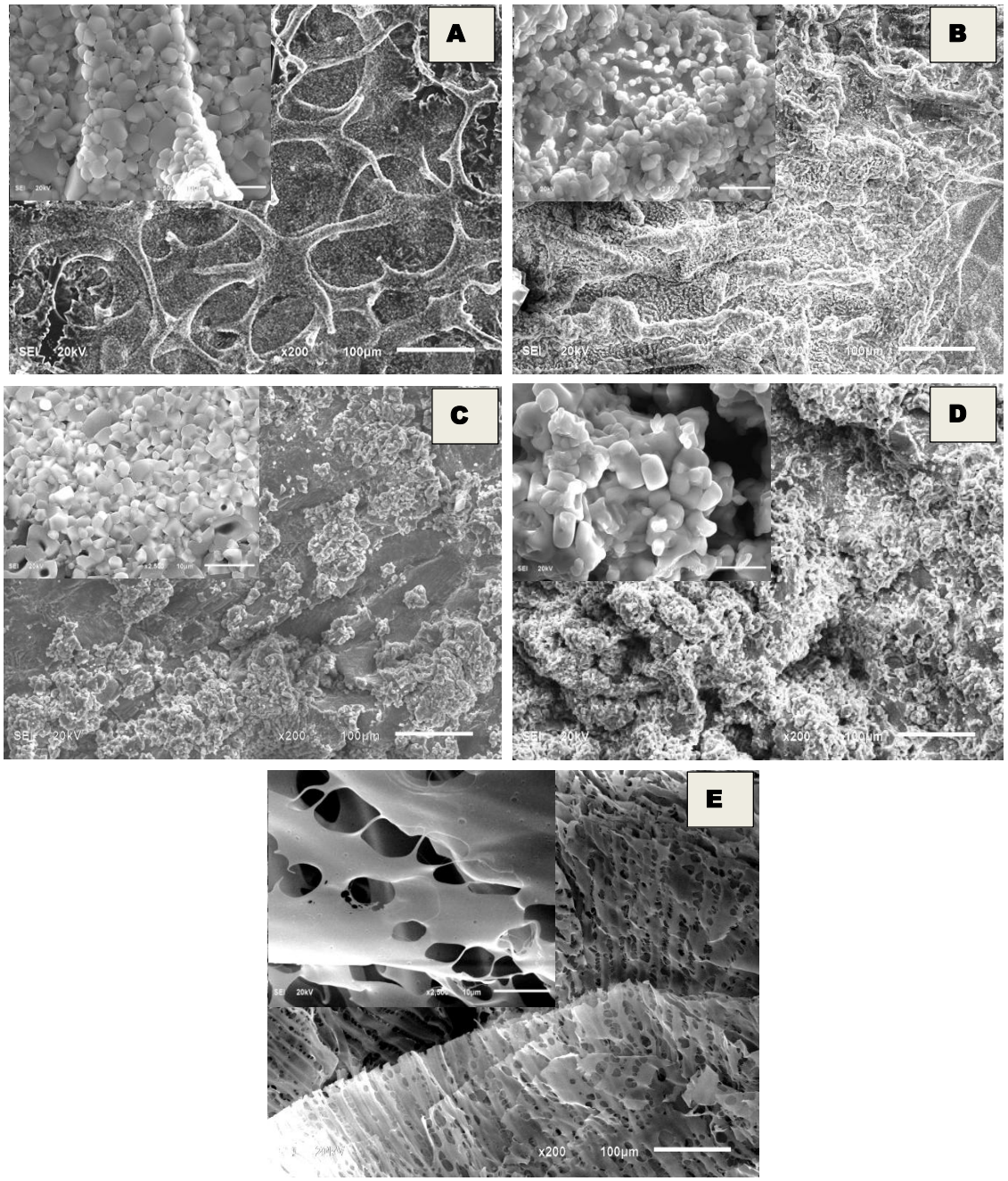

Figure 2. SEM micrographs of the surface morphology of porous scaffolds (a) HA immersed in SBF for 3 h, (b) HA immersed in SBF for 6 h, (c) HA immersed in SBF for 12 h, (d) HA immersed in SBF for 18h and only HA

Annals of R.S.C.B., ISSN:1583-6258, Vol. 25, Issue 4, 2021, Pages. 12822 - 12833
Received 05 March 2021; Accepted 01 April 2021.

The EDS was performed to confirm the mineral phase. Figure 3 shows the EDS image of the HA/HAp sponges after 12 h incubation in the SBF. The major elements in the mineralized scaffolds consist of carbon (C), oxygen (O), phosphorus (P) and calcium (Ca). The peaks of carbon and oxygen could be from HA and the phosphorus and calcium could be from the hydroxyapatite mineral phase. The Ca/P ratio is nearly 2, which is similar to the native bone which is 1.67.[26] It has been reported that calcium phosphate present in the scaffold improves the cell response after implantation.[27] This result suggests that bone like apatite has been deposited on the surface of HA sponges.

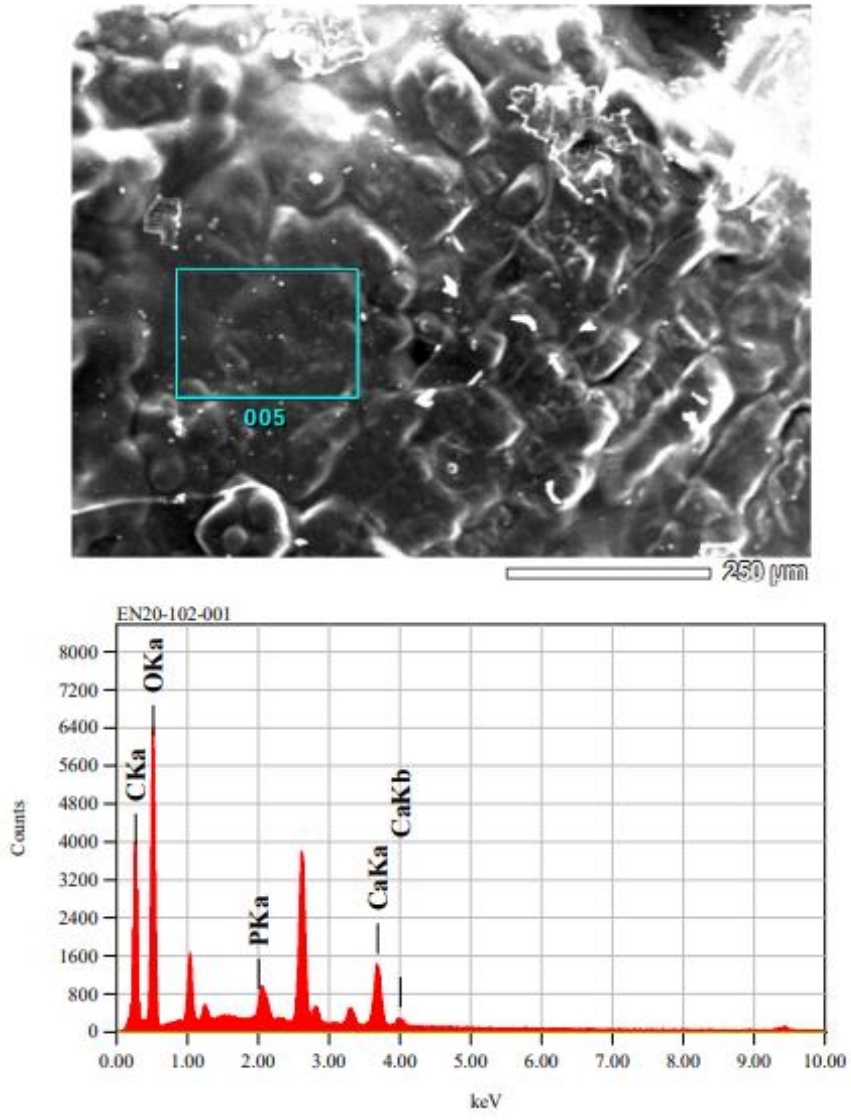

Figure 3. EDS image of the HA/HAp sponges after 12 h incubation in the SBF

3.2. Porosity of scaffolds

One of the most important features to evaluate the biomaterial properties for tissue engineering is the porosity of the scaffolds. Porosity of each material was calculated and the results are tabulated in Table 3. All the sponges were highly porous and the porosity decreased with increase in the mineralization time. The maximum porosity of 95.83 % was observed for 3 h immersion

Annals of R.S.C.B., ISSN:1583-6258, Vol. 25, Issue 4, 2021, Pages. 12822 - 12833
Received 05 March 2021; Accepted 01 April 2021.

and the minimum porosity of 81.42% was shown for the 18 h immersion. This decrease in the porosity might be due to the increase in the deposition of the hydroxyapatite minerals on the walls of the sponges. High material porosity is required for cells and nutrient flow. Usually scaffolds with porosity above 90% are suitable for tissue engineering.[28]The results suggest that these highly porous materials would favor the cell growth and proliferation and make these sponges very special for tissue engineering.

Table 3. Porosity of HA/HAp sponges with different immersion time in SBF solution

S.No	Specimen HA/HAp sponges with different immersion time in SBF	Porosity %
1	3hr	95.83
2	6hr	93.88
3	12hr	92.10
4	18hr	81.42

3.3. ATR-FTIR spectroscopy analysis

Information about the molecular structure of the polymer and the changes involved during the mineralization process in the polymer can be obtained by the infrared spectroscopy from the position and shape of the bands. The FTIR spectra of HA/HAp sponges with different immersion time in SBF solution is shown in Figure 4. All the sponges showed broad peaks around 3400 cm^{-1} to 3450 cm^{-1} due to the abundant –OH groups in the polysaccharide chain. The sharp peaks around 1650 cm^{-1} represented the C=O group of both the amide and carboxylate moieties respectively. The peak value was in the range of 1610 cm^{-1} to 1655 cm^{-1} HA with the highest value of 1655 cm^{-1} for HA/HAp sponges with immersion time of 3 h in SBF solution and lowest value of 1610 cm^{-1} for HA/HAp sponges with immersion time of 18 h in SBF solution.

The carbonate group (CO_3^{2-}) peaks of HAp appear at 1417, 1413, 1417and 1415cm-1 for for 3h , 6h, 12h and 18h of immersion in the SBF solution respectively, suggesting that these are type B carbonate apatite.[20,29] Peaks observed in the range of 1030-1150 cm^{-1} are from hydroxyapatite. FTIR spectra showed characteristic bands at 567, 960 to 1200 cm^{-1} corresponding to $PO4^{3-}$ group of calcium phosphate.[30] The peaks at 3343 cm^{-1} corresponds to the hydroxyl group and peaks at 2900 cm^{-1} and 1300 cm^{-1} are due to the C-H and ether linkage The characteristic absorption bands of PO_4 are formed as P-O stretching at 1041 cm-1 and 1151cm-1 after 3h immersion; 1040 cm-1 and 1141cm-1 after 6h immersion; 1041 cm-1 and 1153cm-1 after 12h immersion; and 1035 cm-1 and 1143cm-1 after 18h immersion.[31]

With increase in the mineralization time the intensity of the absorption bands of PO_4 increased. This shift after mineralization is due to the new bond formation. This is a proof that the bond

Annals of R.S.C.B., ISSN:1583-6258, Vol. 25, Issue 4, 2021, Pages. 12822 - 12833
Received 05 March 2021; Accepted 01 April 2021.

between the polymer HA and HAp involves this group. In conclusion, the presence of HA and HAp showed mix major peaks confirmed the interaction of both polymers HA and HAp.

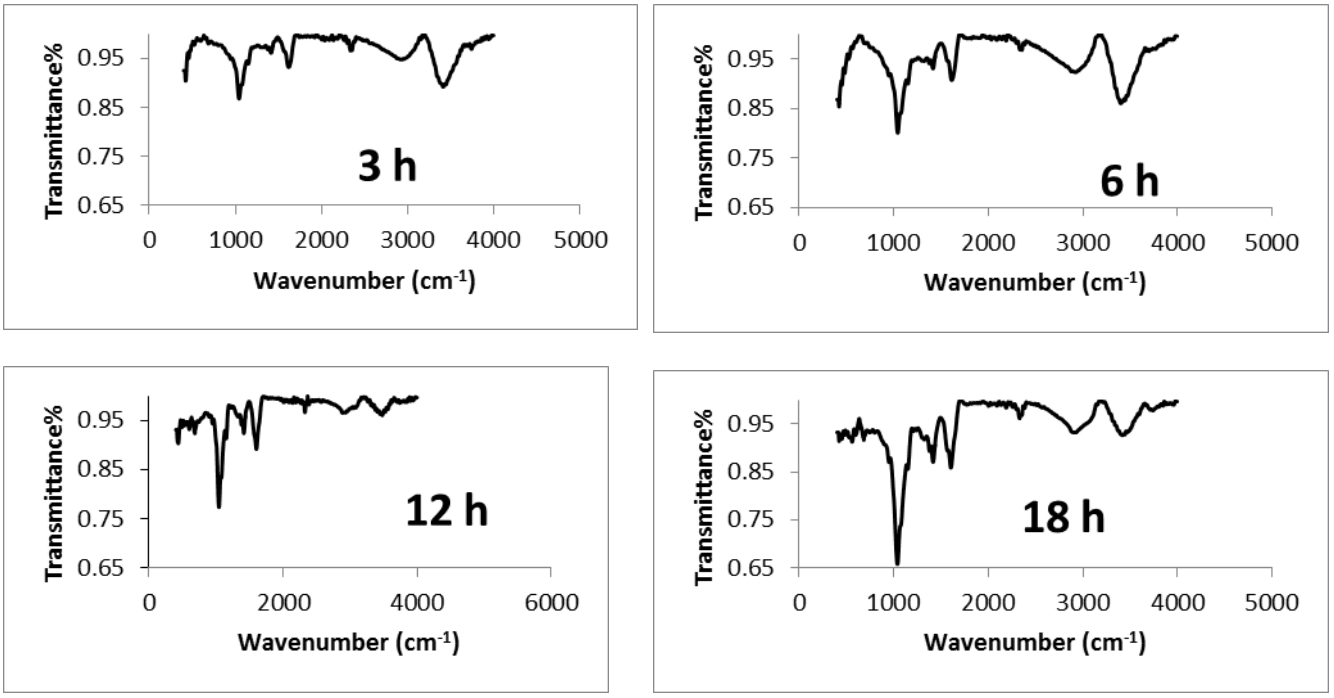

Figure 4. FTIR spectra of HA sponges treated with SBF solution at different time periods. a) 3 h, b) 6 h c) 12 h, d) 18 h and (e) 24 h.

3.4. Thermogravimetric (TGA) studies

Thermal degradation behavior of HA/HAp sponges were analyzed from the TGA curves as shown in Figure 5. And the % mass losses for the sponges are shown in Table 4. The TGA curves indicated significant weight loss for all the HA/HAp sponges when the temperature was increased to 800 °C.

Table 4. The % mass losses for the sponges

Sample	Stage1 weight loss %	Stage1 weight loss %
HA/HAp sponges with 3h immersion in SBF	9.4	30.2
HA/HAp sponges with 6h immersion in SBF	8.9	29.5
HA/HAp sponges with 12h immersion in SBF	8.1	21.6
HA/HAp sponges with 18h immersion in SBF	8.0	20.18

The sponges showed the presence of three stages of weight loss when the immersion time was less (3h and 6h) and two stages when the immersion time was increased to 12h or 18h. The presence of three stages suggest that there are more than one degradation process.[32] In the first stage, the sponges showed lower values of % weight loss which was 9.41%, 8.9%, 8.1% and

Annals of R.S.C.B., ISSN:1583-6258, Vol. 25, Issue 4, 2021, Pages. 12822 - 12833
Received 05 March 2021; Accepted 01 April 2021.

8.0% for 3h , 6h, 12h and 18h of immersion in the SBF solution respectively. The weight loss in the second stage was more significant around 30.2%, 29.5%, 21.6% and 20.18% for 3h, 6h, 12h and 18h of immersion in the SBF solution respectively. In the second stage, the onset of the weight loss for the different HA/HAp sponges were 209 °C, 217 °C, 225 °C and 229 °C for 3h , 6h, 12h and 18h of immersion in the SBF solution respectively. The weight loss in the first stage around 21.4 °C -229 °C is due to the evaporation of water bound to the HA/HAp sponges and also due to the volatilization of small molecules from the sponges.[8] The weight loss in the second stage is due to the physical transition or the chemical degradation of the HA/Hap sponges as a result of C-C bond scission.[32] Overall the thermal stability increased with increase in the immersion time of the HA sponges in the SBF solution that results in the increase of the hydroxyapatite mineralization.

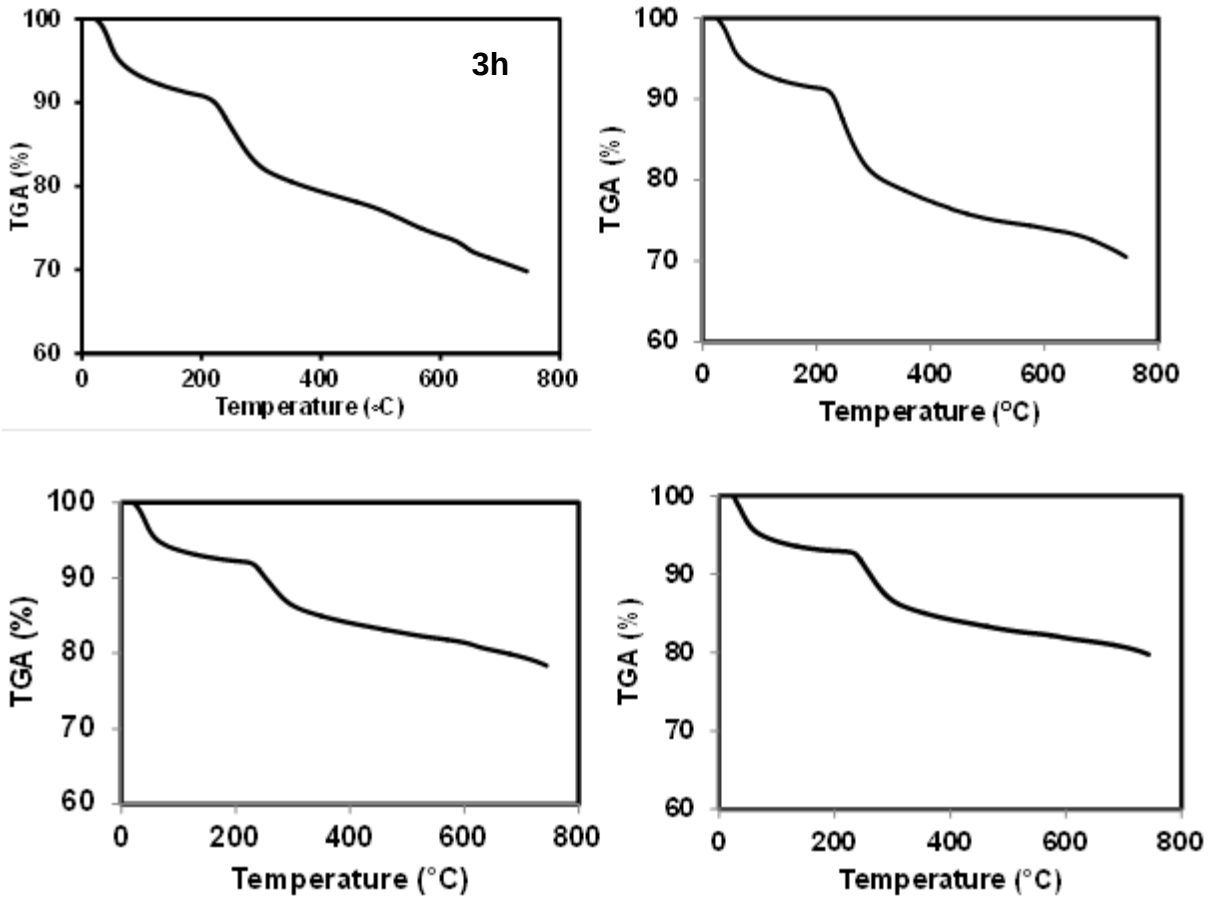

Figure 5. TGA analysis for HA/HAp sponges with different immersion time in SBF solution(a) 3h, (b) 6h (c) 12h and (d) 18h.

3.5. X-ray diffraction

The crystallinity of the hydroxyapatite deposited was characterized by XRD analysis. Figure 6 shows the XRD pattern of HA/HAp sponges with different immersion time in SBF solution(a) 3h, (b) 6h (c) 12h and (d) 18h. The major peaks appeared at 2θ angle = 26.93, 31.37 and 45.15°

Annals of R.S.C.B., ISSN:1583-6258, Vol. 25, Issue 4, 2021, Pages. 12822 - 12833
Received 05 March 2021; Accepted 01 April 2021.

related to (002), (211) and (222) planes, which refers to a good crystallization for hydroxyapatite phase[33, 34.]

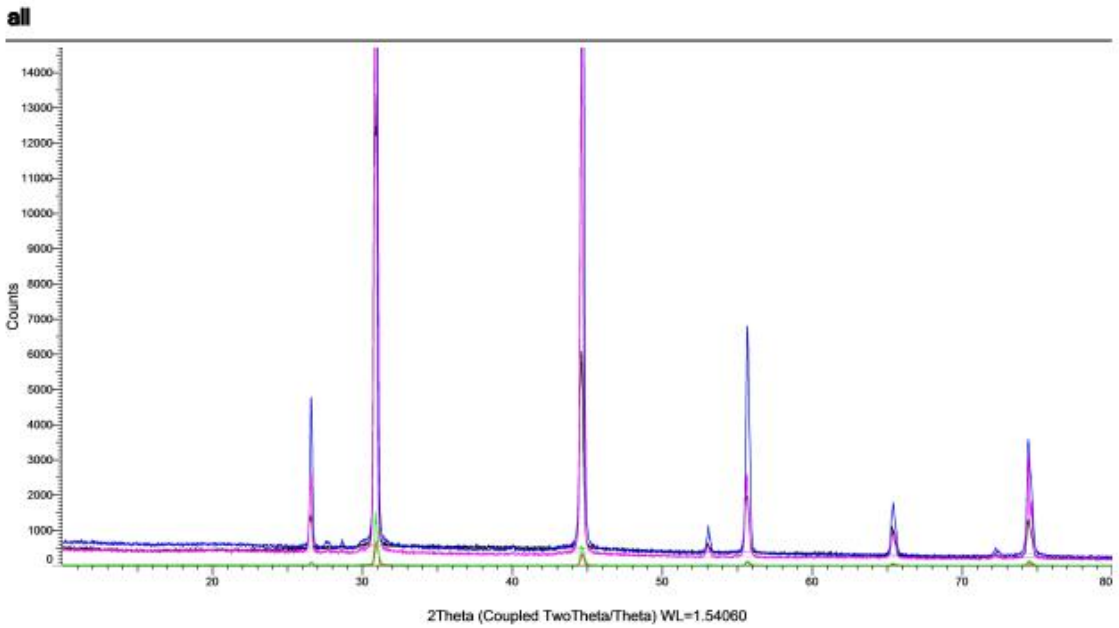

Figure 6. X-ray diffraction patterns of HA/HAp sponges with different immersion time in SBF solution(a) 3h, (b) 6h (c) 12h and (d) 18h.

4. Conclusion

Porous hyaluronic acid sponges cross-linked with BDDE were fabricated using freeze-drying technique. Highly stable HA/HAp sponges were obtained by immersing the HA sponges in SBF solution at different periods of time. The HA and the HA/HAp sponges showed interconnected porous structure with diameter in the range of (100–300 μm) and (0.5–5.0 μm) respectively. With increase in the mineralization time the pore size decreased this is because of the increase in the coating of the hydroxyapatite on the surface of the pores. The HA/HAp sponges showed high porosity ranging from 85-95 %, which is an important requirement for tissue engineering applications. The HA/HAp sponges were thermally stable. The FTIR and EDS confirmed the formation of hydroxyapatite minerals on HA sponges. The in-situ mineralization of hydroxyapatite was uniform throughout the HA sponges. These HA/HAp sponges will be a promising material for bone tissue engineering.

Acknowledgment

This work was supported by the TRC research grant. The authors acknowledge the support from the department of biological sciences in the Faculty of Arts and Sciences at the University of Nizwa.

Annals of R.S.C.B., ISSN:1583-6258, Vol. 25, Issue 4, 2021, Pages. 12822 - 12833
Received 05 March 2021; Accepted 01 April 2021.

References

[1] Ullah S and Chen X. Fabrication, applications and challenges of natural biomaterials in tissue engineering. Appl Mater Today 2020; 20: 100656.

[2] Subramaniam S, Fang YH, Sivasubramanian S, et al. Hydroxyapatite-calcium sulfate-hyaluronic acid composite encapsulated with collagenase as bone substitute for alveolar bone regeneration. Biomaterials 2016; 74: 99-108.

[3] Zulkifli FH, Hussain FS J, Harun WSW, et al. Highly porous of hydroxyethyl cellulose biocomposite scaffolds for tissue engineering. Int J Bio Macromol 2019; 122: 562-571.

[4] Chahal S, Fathima SJH, and Yusoff MBM. Biomimetic growth of bone-like apatite via simulated body fluid on hydroxyethyl cellulose/polyvinyl alcohol electrospunnanofibers. Biomed Mater Eng 2014; 24: 799-806.

[5] Schanté CE, Zuber G, Herlin C, et al. Chemical modifications of hyaluronic acid for the synthesis of derivatives for a broad range of biomedical applications. CarbohydrPolym 2011; 85: 469-489.

[6] Manferdini C, Guarino V, Zini N, et al. Mineralization behavior with mesenchymal stromal cells in a biomimetic hyaluronic acid-based scaffold. Biomaterials 2010; 31: 3986-3996.

[7] Pedron S, Becka E and Harley BA. Regulation of glioma cell phenotype in 3D matrices by hyaluronic acid. Biomaterials 2013; 34: 7408-7417.

[8] Kaczmarek B, Sionkowska A, Gołyńska M, etal.In vivo study on scaffolds based on chitosan, collagen, and hyaluronic acid with hydroxyapatite. Int J Bio Macromol 2018; 118: 938-944.

[9] Wang TW, Sun JS, Wu HC, et al. The effect of gelatin–chondroitin sulfate–hyaluronic acid skin substitute on wound healing in SCID mice. Biomaterials 2006; 27: 5689-5697.

[10] Garcia-Fuentes M, Meinel AJ, Hilbe M, et al. Silk fibroin/hyaluronan scaffolds for human mesenchymal stem cell culture in tissue engineering. Biomaterials 2009; 30: 5068-5076.

[11] Yan S, Zhang Q, Wang J, et al. Silk fibroin/chondroitin sulfate/hyaluronic acid ternary scaffolds for dermal tissue reconstruction. ActaBiomaterialia 2013; 9: 6771-6782.

[12] Florczyk SJ, Wang K, Jana S, et al. Porous chitosan-hyaluronic acid scaffolds as a mimic of glioblastoma microenvironment ECM. Biomaterials 2013; 34: 10143-10150.

[13] Lee GH, Makkar P, Paul K, et al. Incorporation of BMP-2 loaded collagen conjugated BCP granules in calcium phosphate cement based injectable bone substitutes for improved bone regeneration. Mater SciEng C 2017; 77: 713-724.

[14] Huang R, Zhu X, Tu H, et al. The crystallization behavior of porous poly (lactic acid) prepared by modified solvent casting/particulate leaching technique for potential use of tissue engineering scaffold. Mater Lett 2014; 136:126-9.

[15] Wang S, Hu F, Li J, et al. Design of electrospunnanofibrous mats for osteogenic differentiation of mesenchymal stem cells. NanomedNanotechnol 2018; 14: 2505-2520.

[16] Shahbazarab Z, Teimouri A, Chermahini AN, et al. Fabrication and characterization of nanobiocomposite scaffold of zein/chitosan/nanohydroxyapatite prepared by freeze-drying method for bone tissue engineering. Int J Bio Macromol 2018; 108: 1017-1027.

[17] Abzan N, Kharaziha M, Labbaf S, et al. Modulation of the mechanical, physical and chemical properties of polyvinylidene fluoride scaffold via non-solvent induced phase separation process for nerve tissue engineering applications. EurPolymJ 2018; 104: 115-27.

[18] Leon CA. New perspectives in mercury porosimetry. Adv Colloid Interface Sci 1998; 76–77:

341–72.

[19] Kaczmarek B, Sionkowska A and Osyczka AM. The application of chitosan/collagen/hyaluronic acid sponge cross-linked by dialdehyde starch addition as a matrix for calcium phosphate in situ precipitation. Int J Bio Macromol 2018;107: 470-477.

[20] Tas AC and Bhaduri SB. Rapid coating of Ti6Al4V at room temperature with a calcium phosphate solution similar to 10× simulated body fluid. J Mater Res 2004; 19: 2742-2749.

[21] Mavis B, Demirtaş TT, Gümüşderelioğlu M, et al. Synthesis, characterization and osteoblastic activity of polycaprolactonenanofibers coated with biomimetic calcium phosphate. ActaBiomater 2009; 5: 3098-3111.

[22] Beşkardeş IG and Gümüşderelioğlu M. Biomimetic apatite-coated PCL scaffolds: effect of surface nanotopography on cellular functions. J BioactCompatPolym 2009; 24: 507-24.

[23] Ma L, Gao C, Mao Z, et al. Collagen/chitosan porous scaffolds with improved biostability for skin tissue engineering. Biomaterials 2003; 24: 4833-4841.

[24] Liu X, Smith LA, Hu J, et al. Biomimetic nanofibrous gelatin/apatite composite scaffolds for bone tissue engineering. Biomaterials 2009; 30: 2252-2258.

[25] Wang TW and Spector M. Development of hyaluronic acid-based scaffolds for brain tissue engineering. ActaBiomater 2009; 5: 2371-2384.

[26] Raynaud S, Champion E, Bernache-Assollant D, et al. Calcium phosphate apatites with variable Ca/P atomic ratio I. Synthesis, characterisation and thermal stability of powders. Biomaterials 2002; 23: 1065-1072.

[27] Xu HH and Simon Jr CG. Fast setting calcium phosphate–chitosan scaffold: mechanical properties and biocompatibility. Biomaterials 2005; 26: 1337-1348.

[28] Nguyen TBL and Lee BT. A combination of biphasic calcium phosphate scaffold with hyaluronic acid-gelatin hydrogel as a new tool for bone regeneration. Tissue Eng Part A 2014; 20: 1993-2004.

[29] Coates J. Encyclopedia of analytical chemistry: interpretation of infrared spectra, a practical approach. R.R. Meyers (Ed.), Encyclopedia of Analytical Chemistry, John Wiley and Sons Ltd., Chichester, UK (2000), 10815-10837.

[30] Idowu B, Cama G, Deb S, et al. In vitro osteoinductive potential of porous monetite for bone tissue engineering. J Tissue Eng 2014; 5: 1-14.

[31] LeGeros RZ. Biodegradation and bioresorption of calcium phosphate ceramics. Clin mater 1993; 14: 65-88.

[32] Guirguis, O. W, Moselhey, M. T. Thermal and structural studies of poly (vinyl alcohol) and hydroxypropyl cellulose blends. Natural Science 2012;.4, No.1, 57-67.

[33] F. Ghorbani, et al, Bioactive and biostable hyaluronic acid-pullulan dermal hydrogels incorporated with biomimetic hydroxyapatite spheres. Mater.Sci and EngC 112 (2020) 110609, 1-13.

[34] K. M. Tohamy, et al. Novel alginate/hydroxyethyl cellulose/hydroxyapatite composite scaffold for bone regeneration: In vitro cell viability and proliferation of human mesenchymal stem cells. Int J Bio Macromol2018; 118: 448-460.